Enzymic Analysis of the Crabtree Effect in Glucose-Limited Chemostat Cultures of *Saccharomyces cerevisiae*

ERIK POSTMA,* CORNELIS VERDUYN, W. ALEXANDER SCHEFFERS, AND JOHANNES P. VAN DIJKEN

Department of Microbiology, Delft University of Technology, Julianalaan 67, 2628 BC Delft, The Netherlands

The physiology of *Saccharomyces cerevisiae* CBS 8066 was studied in glucose-limited chemostat cultures. Below a dilution rate of 0.30 h^{-1} glucose was completely respired, and biomass and CO_2 were the only products formed. Above this dilution rate acetate and pyruvate appeared in the culture fluid, accompanied by disproportional increases in the rates of oxygen consumption and carbon dioxide production. This enhanced respiratory activity was accompanied by a drop in cell yield from 0.50 to 0.47 g (dry weight) g of glucose^{-1}. At a dilution rate of 0.38 h^{-1} the culture reached its maximal oxidation capacity of 12 mmol of O_2 g (dry weight)$^{-1}$ h^{-1}. A further increase in the dilution rate resulted in aerobic alcoholic fermentation in addition to respiration, accompanied by an additional decrease in cell yield from 0.47 to 0.16 g (dry weight) g of glucose^{-1}. Since the high respiratory activity of the yeast at intermediary dilution rates would allow for full respiratory metabolism of glucose up to dilution rates close to μ_{max}, we conclude that the occurrence of alcoholic fermentation is not primarily due to a limited respiratory capacity. Rather, organic acids produced by the organism may have an uncoupling effect on its respiration. As a result the respiratory activity is enhanced and reaches its maximum at a dilution rate of 0.38 h^{-1}. An attempt was made to interpret the dilution rate-dependent formation of ethanol and acetate in glucose-limited chemostat cultures of *S. cerevisiae* CBS 8066 as an effect of overflow metabolism at the pyruvate level. Therefore, the activities of pyruvate decarboxylase, NAD$^+$- and NADP$^+$-dependent acetaldehyde dehydrogenases, acetyl coenzyme A (acetyl-CoA) synthetase, and alcohol dehydrogenase were determined in extracts of cells grown at various dilution rates. From the enzyme profiles, substrate affinities, and calculated intracellular pyruvate concentrations, the following conclusions were drawn with respect to product formation of cells growing under glucose limitation. (i) Pyruvate decarboxylase, the key enzyme of alcoholic fermentation, probably already is operative under conditions in which alcoholic fermentation is absent. The acetaldehyde produced by the enzyme is then oxidized via acetaldehyde dehydrogenases and acetyl-CoA synthetase. The acetyl-CoA thus formed is further oxidized in the mitochondria. (ii) Acetate formation results from insufficient activity of acetyl-CoA synthetase, required for the complete oxidation of acetate. Ethanol formation results from insufficient activity of acetaldehyde dehydrogenases. The observed pattern of metabolite production in chemostat cultures is in agreement with the conditions under which these insufficiencies can be calculated to occur. The uncoupling effect of weak acids on respiration and the associated triggering of alcoholic fermentation were confirmed in chemostat experiments in which the yeast was grown in the presence of propionate. In this case, the maximal respiratory activity was attained at a dilution rate of 0.30 h^{-1}, above which alcoholic fermentation occurred.

The yeast *Saccharomyces cerevisiae* can ferment glucose to ethanol. Under anaerobic conditions, this is the only mode of energy production. In the presence of oxygen, respiration occurs. However, alcoholic fermentation may set in even under aerobic conditions (50) if the glucose concentration surpasses a critical threshold value (53).

Chemostat cultivation is the method of choice to demonstrate this so-called Crabtree effect in yeasts (14, 15, 18), i.e., the occurrence of alcoholic fermentation despite aerobic conditions (50). In glucose-limited chemostat cultures, strictly oxidative metabolism is observed at low dilution rates. When a critical dilution rate is surpassed, alcoholic fermentation is triggered. As a consequence, the amount of biomass produced per unit of substrate consumed decreases drastically (3, 18, 39, 43, 55). Originally this shift in metabolism to alcoholic fermentation in glucose-limited chemostat cultures was believed to result from glucose repression; at high dilution rates, characterized by elevated residual glucose concentrations, a progressive decrease in the specific oxygen consumption rate was observed, accompanied by alterations in components of the respiratory chain and by the

repression of several tricarboxylic acid cycle enzymes (8, 40, 58). However, Barford et al. (5) showed that the phenomena observed by von Meyenburg (55) were transient; after a long adaptation period, *S. cerevisiae* cultures adapted to a permanent steady state in which respiration was not repressed but rather occurred at a maximal rate which was independent of the dilution rate. The present view is that the occurrence of alcoholic fermentation in aerobic sugar-limited cultures of *S. cerevisiae* growing at high dilution rates is a consequence of the limited respiratory capacity of this yeast, resulting in overflow metabolism at the pyruvate level (28, 39).

In this paper evidence is presented that the dilution rate-dependent metabolic transition of steady-state cultures of *S. cerevisiae* is not abrupt. At intermediary growth rates, steady-state cultures of *S. cerevisiae* CBS 8066 exhibit an unexpectedly high rate of respiration, probably caused by the uncoupling effect of weak organic acids produced by the organism. The production of these metabolites (acids) as a function of the dilution rate results from overflow metabolism at two branching points in glucose metabolism (Fig. 1). At the level of pyruvate, respiration competes with alcoholic fermentation via the mitochondrial pyruvate dehydrogenase

---

* Corresponding author.

glucose

pyruvate ▸ acetaldehyde ▸ ethanol
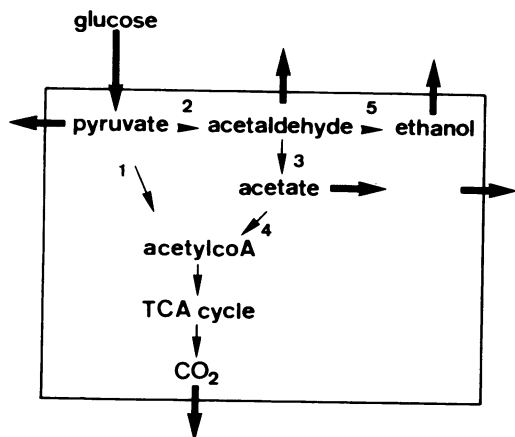
acetate ➝

acetylcoA

TCA cycle

CO_2

FIG. 1. Alternative routes of pyruvate catabolism in yeasts. The enzymes catalyzing the various reactions are indicated as follows: 1, pyruvate dehydrogenase complex; 2, pyruvate decarboxylase; 3, acetaldehyde dehydrogenase (NAD^+ or $NADP^+$ linked); 4, acetyl-CoA synthetase; 5, alcohol dehydrogenase. TCA, Tricarboxylic acid.

complex and the cytosolic pyruvate decarboxylase (24, 25). Once formed through the activity of pyruvate decarboxylase, acetaldehyde may feed the tricarboxylic acid cycle via acetate and acetyl coenzyme A (acetyl-CoA) (25, 27, 35). Alternatively, instead of being oxidized to carbon dioxide, acetaldehyde may be reduced to ethanol (24, 50, 52).

In view of the characteristic pattern of overflow metabolism in glucose-limited chemostat cultures of *S. cerevisiae* CBS 8066, it was of interest to relate the excretion of the various intermediates to the activities of enzymes catalyzing their formation or degradation (Fig. 1).

MATERIALS AND METHODS

Microorganism and growth conditions. *S. cerevisiae* CBS 8066 was maintained on malt agar slopes. The organism was grown under glucose limitation at 30°C in a fermentor as described by Harder et al. (23) with a working volume of 800 ml, a stirrer speed of 700 rpm, and an airflow of 4 liter min^{-1}. The dissolved oxygen tension was higher than 50% air saturation at all dilution rates. The pH was automatically controlled at 5.0 by the addition of 2 M KOH. The medium was prepared as described by Bruinenberg et al. (11) with the following modifications per liter: KH_2PO_4, 3.5 g; $MgSO_4 \cdot 7H_2O$, 0.75 g; $(NH_4)_2SO_4$, 7.5 g; trace element solution, 2 ml; and vitamin solution, 2 ml. The trace element solution used in this study contained 10 times as much $NaMoO_4 \cdot 2H_2O$ as that reported by Bruinenberg et al. (11). The glucose concentration in the reservoir was 15 g $liter^{-1}$.

Like other *S. cerevisiae* strains, in steady-state cultures *S. cerevisiae* CBS 8066 sometimes exhibited oscillations in its metabolic behavior. This phenomenon is due to spontaneous cell synchronization (38, 55). When oscillations occurred, analysis of culture parameters was not performed until they had disappeared.

Determination of dry weight. For dry weight measurements nitrocellulose filters (pore size, 0.45 μm; Gelman Sciences, Inc., Ann Arbor, Mich.) were used. After removal of the medium by filtration, the filters were washed with demineralized water and dried in an R-7400 Magnetron Oven (Sharp Inc., Osaka, Japan) for 15 min. This procedure yielded the same dry weight data as drying of filters at 80°C.

Analysis of oxygen consumption and carbon dioxide production. Oxygen and carbon dioxide were analyzed in the dried gas (Permapure Dryer; Inacom Instruments, Farmingdale, United Kingdom) from the fermentor with an OA-184 oxygen analyzer (Tayler Servomex Ltd., Crowborough, Sussex, United Kingdom) and a carbon dioxide analyzer (Beckman Instruments, Inc., Fullerton, Calif.). The gas flow rate (as measured in the exhaust line) was determined with a water-filled precision gas flow meter (Schlumberger, Dordrecht, The Netherlands). The carbon dioxide production and oxygen consumption rates in the fermentor were calculated according to the following equations:

$$qCO_2 = [(q_{gas, out} \times pCO_{2_{out}}) - (q_{gas, in} \times pCO_{2_{in}})]/V_m$$

$$qO_2 = [(q_{gas, in} \times pO_{2_{in}}) - (q_{gas, out} \times pO_{2_{out}})]/V_m$$

$$q_{gas, in} = [(1 - pCO_{2_{out}} - pO_{2_{out}}) \times q_{gas, out}]/0.79$$

In these equations qCO_2 and qO_2 represent the carbon dioxide production and oxygen consumption rates (moles $hour^{-1}$); q_{gas} represents the gas flow rates (liter $hour^{-1}$); V_m is the molar volume (liters) at atmospheric pressure and room temperature; and pO_2 and pCO_2 represent the volume fractions of oxygen and carbon dioxide.

Analysis of metabolites. Rapid sampling of culture fluid was performed as described by Postma et al. (42). Spectrophotometric assays were performed at 30°C with a model 100-60 spectrophotometer (Hitachi Inc., Tokyo, Japan). Ethanol was assayed by the colorimetric method of Verduyn et al. (52). Acetate, glycerol, acetaldehyde, and glucose were determined with kits 148261, 148270, 668613, and 676543, respectively, from Boehringer GmbH, Mannheim, Federal Republic of Germany. The assay mixture for the determination of pyruvate consisted of 100 mM potassium phosphate (pH 7.6), 0.30 mM NADH, 1.5 mM EDTA, and sample. The concentration of pyruvate was calculated from the decrease in extinction at 340 nm following the addition of 2 U of lactate dehydrogenase (EC 1.1.1.27) from Boehringer.

Protein determination. Protein was determined by the Lowry method (35a) with bovine serum albumin (fatty acid free; Sigma Chemical Co., St. Louis, Mo.) as the standard.

Preparation of cell extracts. Samples of steady-state cultures were harvested by low-speed centrifugation, washed twice with 10 mM potassium phosphate buffer (pH 7.5) containing 2 mM EDTA, concentrated fourfold, and stored at −40°C. Before being assayed, the samples were thawed at room temperature, washed, and suspended in 100 mM potassium phosphate buffer (pH 7.5) containing 2 mM $MgCl_2$ and 1 mM dithiothreitol. Extracts were prepared by sonication at 0°C for 2 min at 0.5-min intervals with a 150-W sonicator (MSE, London, United Kingdom). Unbroken cells and debris were removed by centrifugation at 75,000 × g. The supernatant was used as a cell extract.

Enzyme assays. Enzyme activities were assayed immediately after the preparation of the extracts. Spectrophotometric assays were carried out with a model 100-60 spectrophotometer (Hitachi) at 340 nm and 30°C. The reaction velocities were proportional to the amount of enzyme added. The assay mixtures for the individual enzymes are described below.

(i) **Pyruvate decarboxylase (EC 4.1.1.1).** The assay mixture contained imidazole hydrochloride buffer (pH 6.5) (40 mM), $MgCl_2$ (5 mM), thiamine pyrophosphate (0.2 mM), NADH (0.15 mM), and alcohol dehydrogenase (Boehringer) (88 U). The reaction was started with 50 mM pyruvate.
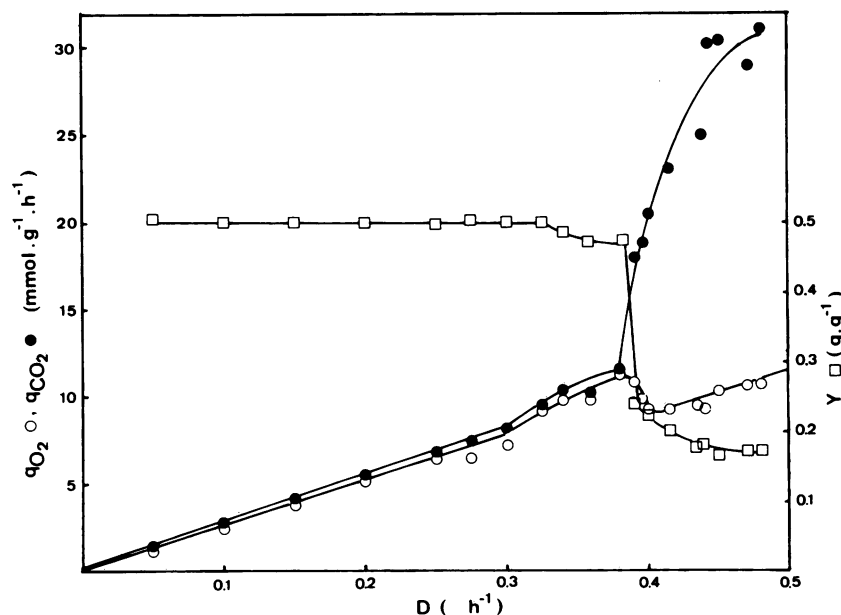
FIG. 2. Specific rates of oxygen uptake (○) and carbon dioxide production (●) and cell yield (□) (gram [dry weight] gram of glucose^{-1}) as a function of the dilution rate in glucose-limited cultures of *S. cerevisiae* CBS 8066.

(ii) Alcohol dehydrogenase (EC 1.1.1.1). The assay mixture contained glycine-KOH buffer (pH 9.0) (50 mM) and NAD$^+$ (1 mM). The reaction was started with 100 mM ethanol.

(iii) Acetaldehyde dehydrogenases (NAD$^+$ and NADP$^+$) (EC 1.2.1.5 and EC 1.2.1.4, respectively). The assay mixture contained potassium phosphate buffer (pH 8.0) (100 mM), pyrazole (15 mM), dithiothreitol (0.4 mM), KCl (10 mM), and NAD$^+$ or NADP$^+$ (0.4 mM). The reaction was started with 0.1 mM acetaldehyde.

(iv) Acetyl-CoA synthetase (EC 6.2.1.1). For the determination of this enzyme the solutions in the Boehringer acetate kit (148261) were used. The reaction mixture consisted of solution 1 (0.3 ml), solution 2 (0.06 ml), malate dehydrogenase (3 U), citrate synthase (0.4 U), and cell extract in a final volume of 1 ml. The reaction was started with 10 mM potassium acetate.

(v) Glucose 6-phosphate dehydrogenase (EC 1.1.1.49). The assay mixture contained Tris hydrochloride buffer (pH 8.0) (50 mM), MgCl$_2$ (5 mM), and NADP$^+$ (0.4 mM). The reaction was started with 5 mM glucose 6-phosphate.

RESULTS

Oxygen consumption and carbon dioxide production rates in steady-state cultures. In contrast to *S. cerevisiae* LBG H1022, the strain originally used by von Meyenburg (H. K. von Meyenburg, Ph.D. thesis, Technische Hochschule, Zürich, Switzerland, 1969) and Rieger et al. (43), which starts to ferment at $D = 0.30$ h^{-1}, our strain exhibited a fully "respiratory" metabolism (no ethanol formation) up to a dilution rate of 0.38 h^{-1} (Fig. 2). Between dilution rates of 0.30 and 0.38 h^{-1}, however, caution had to be taken when increasing the dilution rate. A sudden increase in the dilution rate of more than 0.02 h^{-1} triggered alcoholic fermentation, and the culture required far more than 5 volume changes to reach a new steady state with full respiratory metabolism. This phenomenon was originally observed by Barford et al. (5).

Up to $D = 0.30$ h^{-1} glucose was fully respired by *S. cerevisiae* CBS 8066, leading only to CO$_2$ and biomass

formation. The O$_2$ consumption and CO$_2$ production rates increased linearly with the dilution rate. Above $D = 0.30$ h^{-1}, however, disproportional increases in qO$_2$ and qCO$_2$ were observed (Fig. 2) and were accompanied by a significant drop in biomass yield from 0.50 to 0.47 g (dry weight) g of glucose^{-1}. At $D = 0.38$ h^{-1} the maximal oxygen consumption rate was observed: 12 mmol of O$_2$ g (dry weight)$^{-1}$ h^{-1}. At higher dilution rates, alcoholic fermentation occurred, as was evident from the profiles of oxygen consumption and carbon dioxide production (enhanced carbon dioxide production rates were caused by fermentation). The rate of oxygen consumption by the culture above $D = 0.38$ h^{-1} followed a peculiar pattern. It decreased from 12 mmol g^{-1} h^{-1} at $D = 0.39$ h^{-1} to 9 mmol g^{-1} h^{-1} at $D = 0.41$ h^{-1}. A further increase in the dilution rate to 0.48 h^{-1} again resulted in an increase in the qO$_2$, leading to a qO$_2$ of 10.7 mmol g^{-1} h^{-1}.

Metabolite production in steady-state cultures. Analysis of the culture fluid revealed that glycerol was present at all dilution rates tested, but its concentration increased at higher dilution rates (Fig. 3A). Pyruvate, the end product of glycolysis at the branching point of the oxidative and fermentative routes, appeared at dilution rates above 0.30 h^{-1} (Fig. 3A). Acetate followed essentially the same pattern as pyruvate (Fig. 3B). As expected, ethanol formation did set in at $D = 0.39$ h^{-1}, when enhanced CO$_2$ production was observed (Fig. 2). This ethanol formation was accompanied by the appearance of acetaldehyde in the culture (Fig. 3B).

Transient-state responses in respiration. To assess which parameter is decisive for the onset of fermentation in steady-state cultures, we monitored the metabolic behavior of the yeast during dilution rate shift experiments (Fig. 4A). At zero time the culture was shifted from $D = 0.36$ to 0.38 h^{-1}. This shift resulted in a rapid increase in qO$_2$ and qCO$_2$, accompanied by a decrease in biomass yield. However, the observed changes were transient, and the culture adapted to a new steady state with higher qO$_2$ and qCO$_2$ values and a slightly decreased biomass yield. When the dilution rate was shifted to 0.39 h^{-1} a similar pattern was observed, but in this
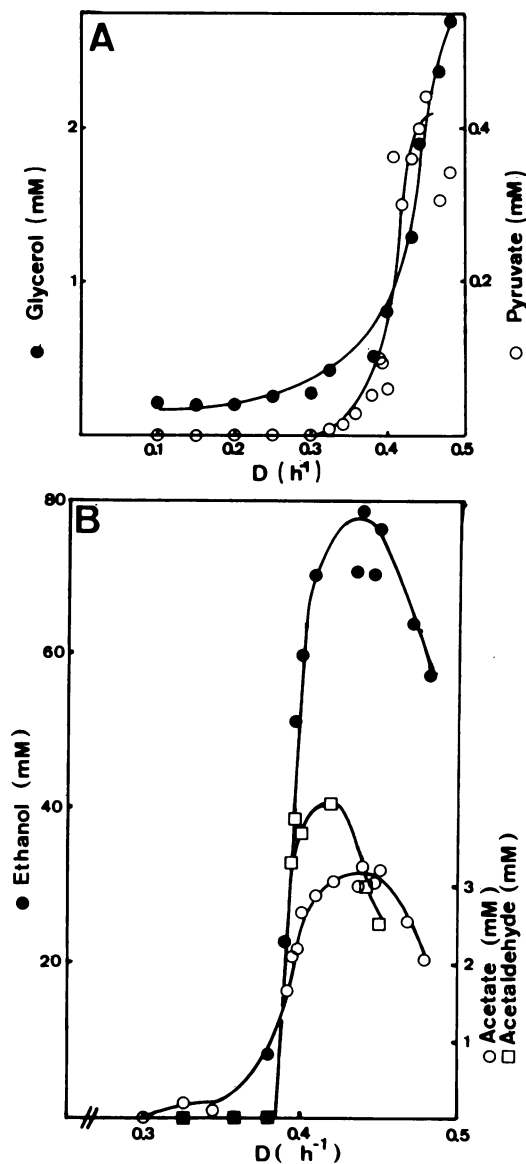
FIG. 3. Steady-state concentrations of the following in glucose-limited chemostat cultures of *S. cerevisiae* CBS 8066: A, pyruvate (○) and glycerol (●); B, ethanol (●), acetate (○), and acetaldehyde (□).

case the decrease in cell yield continued and became permanent. A new steady state after this shift in the dilution rate was only obtained after 25 to 30 volume changes. The maximal qO_2 observed was 12 mmol of O_2 g (dry weight)$^{-1}$ h^{-1}.

Metabolite production in transient-state cultures. The shift in the dilution rate to 0.38 h^{-1} resulted in a transient increase in the glucose concentration from 110 to 280 μM, but after 5 volume changes a new steady state was obtained without alcoholic fermentation (Fig. 4B). Increasing the dilution rate to 0.39 h^{-1} resulted in ethanol formation at residual glucose concentrations that were initially lower than those observed transiently after the shift in the dilution rate from 0.36 to 0.38 h^{-1} (Fig. 4B). The glucose concentration in the culture is thus not the primary cause for ethanol formation. The acetate concentration increased when the dilution rate was

increased. At D = 0.38 h^{-1} a steady-state concentration of 0.6 mM was obtained. A further increase in the dilution rate to 0.39 h^{-1} resulted in an acetate concentration of 2 mM (Fig. 4B).

Enzyme levels in steady-state cultures. Pyruvate decarboxylase, the key enzyme of alcoholic fermentation, was present at high levels at all dilution rates. Above D = 0.38 h^{-1} (at which alcoholic fermentation occurred) a twofold increase to approximately 1 U mg of protein^{-1} was observed, and this level was maintained up to growth rates approaching μ_{max} (Fig. 5A). The activity of alcohol dehydrogenase decreased almost linearly with increasing dilution rates up to 0.39 h^{-1} and then increased again. This peculiar decrease in enzyme activity, which has also been observed for *S. cerevisiae* LBG H1022 (von Meyenburg, Ph.D. thesis), probably results from the existence of various isoenzymes with different sensitivities to glucose repression (36, 58). The increase in alcohol dehydrogenase at high dilution rates is probably attributable to an increase in the fermentative (ethanol-producing) isoenzyme.

NAD$^+$-linked acetaldehyde dehydrogenase activity decreased linearly with increasing dilution rates. Above D = 0.44 h^{-1}, the enzyme was not detectable. A similar decrease was observed for NADP$^+$-dependent acetaldehyde dehydrogenase activity, but this activity was present at all dilution rates tested (Fig. 5B) (13).

Acetyl-CoA synthetase decreased with increasing dilution rates and reached a basal level of 0.02 U mg of protein^{-1} at high dilution rates (Fig. 5C). Glucose 6-phosphate dehydrogenase, the key enzyme for NADPH formation in yeasts (12, 33), slightly increased but then strongly decreased above D = 0.40 h^{-1}.

Affinity constants of enzymes. When two enzymes compete for the same substrate, the affinity constant may be a decisive parameter for the metabolic fluxes via these enzymes (24). At the level of pyruvate, large differences exist in the affinity constants. The mitochondrial pyruvate dehydrogenase has a much lower affinity constant for pyruvate than does the cytosolic pyruvate decarboxylase (9, 31, 34). The affinity constant of pyruvate decarboxylase depends mainly on the cytosolic phosphate concentration, since this enzyme is allosterically inhibited by phosphate (9, 50). Therefore, the K_m of pyruvate decarboxylase was determined in the presence of 5 mM phosphate. This concentration has been reported as the cytosolic phosphate concentration in steady-state glycolyzing *S. cerevisiae* cells on the basis of nuclear magnetic resonance measurements (17). The K_m of the enzyme at this phosphate concentration was 6 mM (Table 1). Since the K_m of pyruvate dehydrogenase for pyruvate is approximately 0.40 mM (Table 1) and since pyruvate decarboxylase must be activated by its substrate (26), it is clear that at low pyruvate concentrations pyruvate is preferentially metabolized via the mitochondrial pyruvate dehydrogenase complex.

At the second branching point of the pyruvate dehydrogenase bypass route (Fig. 1) large differences in substrate affinities were encountered. The K_m for both NAD$^+$- and NADP$^+$-linked acetaldehyde oxidation was 6 μM, whereas the K_m of alcohol dehydrogenase was approximately 100-fold higher (Table 1). Thus, once formed via pyruvate decarboxylase, acetaldehyde is preferentially oxidized to acetate. The low affinity of acetyl-CoA synthetase for acetate (Table 1) indicates that relatively high levels of the acid are required to ensure its oxidation via the tricarboxylic acid cycle.

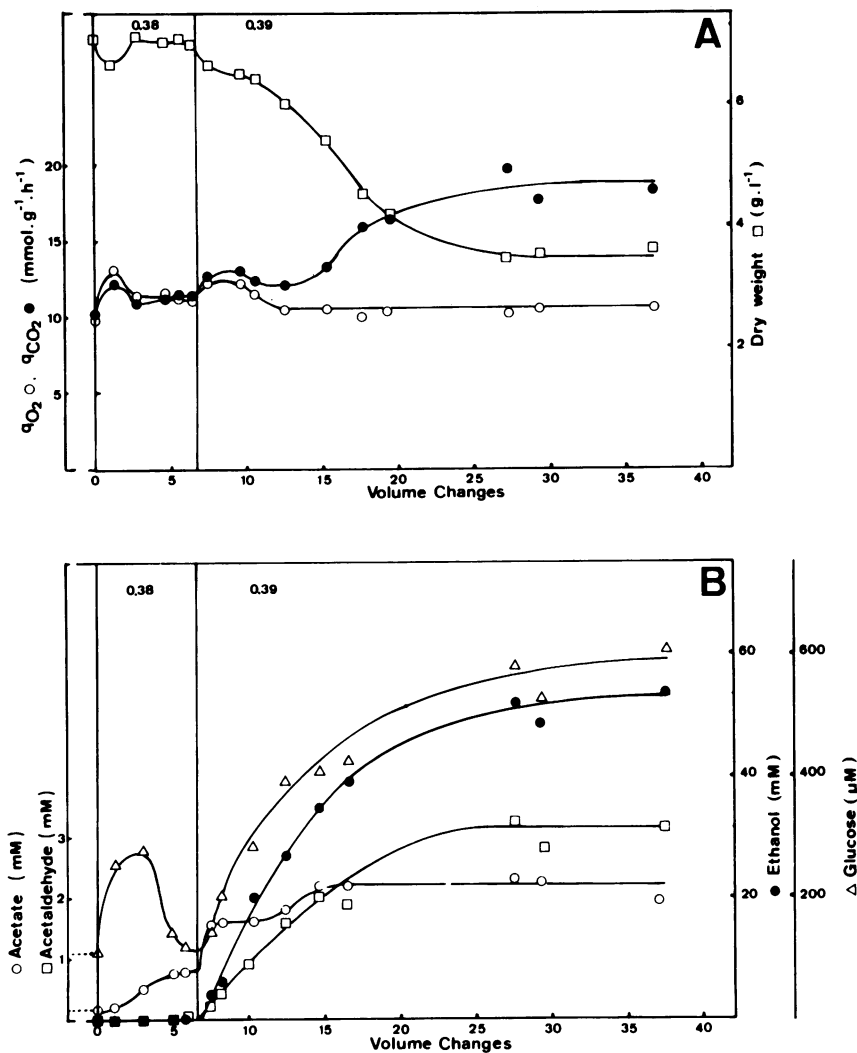**Intracellular pyruvate concentration.** In the culture fluid of

FIG. 4. (A) Specific rates of oxygen uptake (○) and carbon dioxide production (●) and dry weight (□) as a function of the number of volume changes in chemostat cultures of *S. cerevisiae* CBS 8066. (B) Concentrations of glucose (△), acetate (○), acetaldehyde (□), and ethanol (●) as a function of the number of volume changes in chemostat cultures of *S. cerevisiae* CBS 8066. Cultures were shifted in dilution rate from 0.36 to 0.38 h^{-1} and then to 0.39 h^{-1}.

glucose-limited *S. cerevisiae* CBS 8066, pyruvate was detectable above $D = 0.30$ h^{-1} (Fig. 3B). Its concentration increased with increasing dilution rates. The extracellular pyruvate concentration was used to calculate the intracellular concentration on the basis of the assumption that pyruvate accumulates inside the cell as a consequence of the pH gradient over the plasma membrane. The distribution of an acid can be calculated by the following equation:

$$pH_{in} = pK_a + \left(\log_{10}\{[(A_{in}/A_{out})(1 + 10^{pH_{out} - pK_a})] - 1\} \right)$$

in which A_{in} and A_{out} are the concentrations of the anion inside and outside the cell, respectively (1). With this formula and an intracellular pH of approximately 7.0 (16, 17, 37, 49), an extracellular pH of 5.0 (see Materials and Methods), and the pyruvate pK$_a$ of 2.5 (56), an accumulation factor of pyruvate$_{in}$/pyruvate$_{out}$ of 100 was calculated.

Below $D = 0.30$ h^{-1}, extracellular pyruvate concentrations were below the detection limit. Values for these low pyruvate concentrations were obtained via extrapolation of a Hanes plot of the external pyruvate concentrations at dilu-

tion rates between 0.30 and 0.45 h^{-1}. The Hanes plot gave an affinity constant for pyruvate of 9 μM and a D_{max} of 0.45 h^{-1}.

Metabolic fluxes. From the calculated internal pyruvate concentrations at various dilution rates, the enzyme activities in cell extracts, and the affinity constant for pyruvate (Table 1), the in situ pyruvate decarboxylase activity could be calculated with first-order kinetics. For example, at $D = 0.45$ h^{-1} the extracellular concentration was 0.4 mM, pointing to an intracellular concentration of 40 mM (see above). The activity of the enzyme at this dilution rate was 1.0 μmol mg of protein^{-1} min^{-1} (Fig. 5A), and its K_m for pyruvate was 6 mM (Table 1). From the Michaelis-Menten equation it then follows that the in vivo activity of pyruvate decarboxylase is 0.86 μmol mg of protein^{-1} min^{-1} (Fig. 6A), as calculated by the following equation:

$$q = (1.0 \times 40)/(6 + 40)$$

When the capacities (maximal activities) of acetaldehyde dehydrogenases, alcohol dehydrogenase, and acetyl-CoA synthetase were compared with the in situ pyruvate decar-
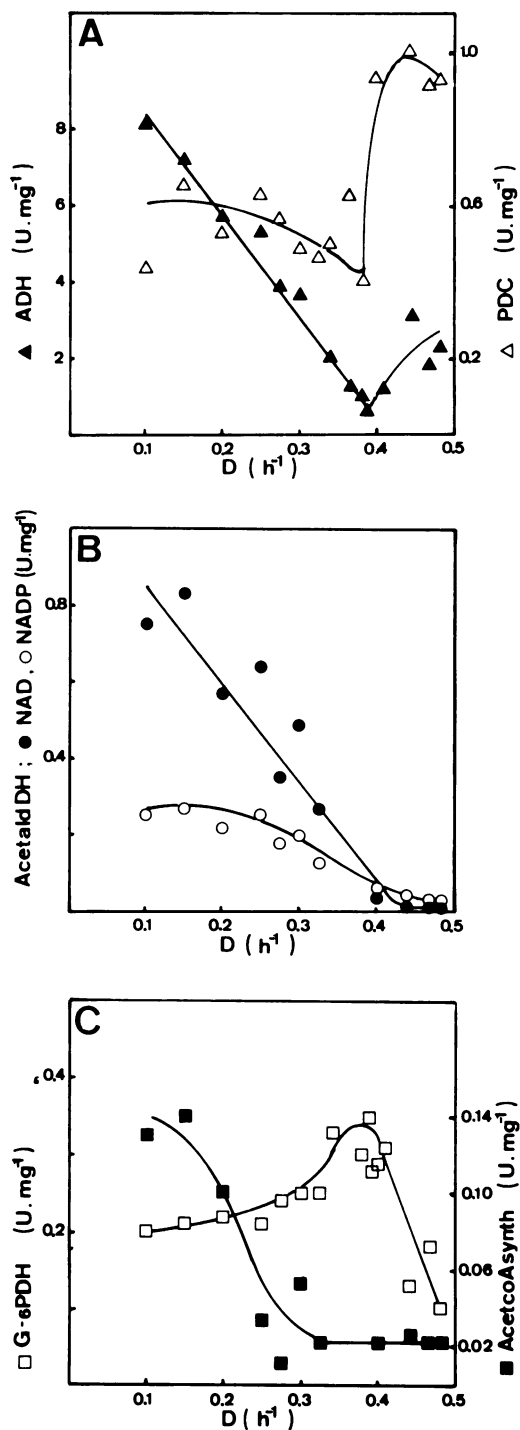
FIG. 5. Specific activities (micromoles milligram of protein^{-1} minute^{-1}) of the following as a function of the dilution rate in glucose-limited chemostat cultures of *S. cerevisiae* CBS 8066: A, alcohol dehydrogenase (▲) and pyruvate decarboxylase (△); B, NAD$^+$ (●)- and NADP$^+$ (○)-dependent acetaldehyde dehydrogenases; C, glucose 6-phosphate dehydrogenase (□) and acetyl-CoA synthetase (■).

boxylase activity, three situations could be defined in glucose-limited cultures of *S. cerevisiae* CBS 8066. Below $D = 0.27$ h^{-1}, the capacities of acetaldehyde dehydrogenases and of acetyl-CoA synthetase were sufficient for converting the

acetaldehyde formed by pyruvate decarboxylase. Between $D = 0.27$ h^{-1} and $D = 0.37$ h^{-1}, however, the capacity of acetyl-CoA synthetase was lower than the rate of production of acetaldehyde via pyruvate decarboxylase, and thus accumulation and excretion of acetate occurred (Fig. 6A and B). At $D = 0.37$ h^{-1}, a second crossover was apparent. At this dilution rate the capacities of both acetyl-CoA synthetase and acetaldehyde dehydrogenases were lower than the calculated in situ pyruvate decarboxylase activity, and thus excretion of ethanol also became a necessity. The capacity of alcohol dehydrogenase (micromoles milligram of protein^{-1} minute^{-1}) (Fig. 5A) was high enough in this respect, particularly if it is taken into consideration that the enzyme assay was performed by measuring ethanol oxidation rather than acetaldehyde reduction. The latter reaction proceeded five times faster under conditions of substrate excess (51). Thus, the capacity of alcohol dehydrogenase at dilution rates at which ethanol production occurred was at least 10-fold in excess over the in situ pyruvate decarboxylase activity (Fig. 5A).

The in situ flux via pyruvate decarboxylase, calculated on the basis of enzyme data, could be correlated with the observed rate of product formation in the chemostat (Fig. 6B). For the conversion of the activities presented in Fig. 6A into activities per unit biomass, an estimated soluble protein content of cells of 33% was used. For example, at $D = 0.45$ h^{-1} the in vivo pyruvate decarboxylase activity equalled 0.86 μmol mg of protein^{-1} min^{-1} (Fig. 6A), corresponding to $0.86 \times (100/33) \times 60 = 17.2$ mmol of acetaldehyde produced g (dry weight)$^{-1}$ h^{-1}. The capacity of acetaldehyde dehydrogenases at this dilution rate was 0.044 μmol mg of protein^{-1} min^{-1}, corresponding to 0.9 mmol of acetate produced g (dry weight)$^{-1}$ h^{-1}. The expected rate of ethanol production, in case acetaldehyde dehydrogenases would operate at saturation, would thus be $17.2 - 0.9 = 16.3$ mmol g (dry weight)$^{-1}$ h^{-1}. Since at this dilution rate ethanol at 75 mM (Fig. 3B) and 2.2 g (dry weight) liter^{-1} (Fig. 2) were present in the culture, the observed rate of ethanol production equalled $75/2.2 \times 0.45 = 15.3$ mmol g (dry weight)$^{-1}$ h^{-1}. It is evident from this example that at high dilution rates ethanol flux was mainly determined by the in vivo pyruvate decarboxylase activity (46), since the capacities of acetaldehyde dehydrogenases were low under these conditions (Fig. 5B and 6A).

In a similar way the maximal rate of acetate production could be calculated by subtracting the capacity of acetyl-CoA synthetase from the calculated flux of acetaldehyde via pyruvate decarboxylase, corrected for the maximal flux via acetaldehyde dehydrogenases. The maximal rate of acetate production was an order of magnitude lower than that of ethanol. The calculated rate was much higher than the rate observed in the chemostat (Fig. 6B). However, in this case a discrepancy between the observed and calculated rates was not surprising, since in the calculation the capacities of several enzymes had to be taken into account, rather than the activity of only pyruvate decarboxylase, as is the case for ethanol production. In addition, the calculation did not include the possible inhibition of acetaldehyde dehydrogenases by acetaldehyde (27). Such inhibition was likely, since the enzyme was inhibited by its substrate above 100 μM (results not shown), whereas the actual acetaldehyde concentrations in the culture were an order of magnitude higher (Fig. 3B).

Effect of propionate on glucose-limited cultures. Weak acids are known to act as uncouplers of the membrane potential when present at high concentrations (2, 7). It was therefore

TABLE 1. Apparent substrate affinity constants (K_ms) of the enzymes of the pyruvate bypass route and of mitochondrial pyruvate oxidation

Enzyme	Substrate	K_m	Reference or source
Pyruvate dehydrogenase	Pyruvate	0.13–0.65 mM	31
Pyruvate decarboxylase	Pyruvate	6 mM	This work
Acetaldehyde dehydrogenase[a]	Acetaldehyde	6 μM	This work
Acetyl-CoA synthetase	Acetate	0.17 mM	19
Alcohol dehydrogenase	Acetaldehyde	0.61 mM	51

[a] With NAD^+ or $NADP^+$ as a cofactor.

investigated whether the increased qO_2 values at dilution rates of 0.30 to 0.38 h^{-1} (Fig. 2) could indeed be attributed to an uncoupling effect of acetate produced by the culture. To this end, propionate, an acid nonmetabolizable by S. cerevisiae, was added to the reservoir medium of a glucose-limited culture at low dilution rates. The addition of propi-

onate resulted in decreased biomass yield and increased qO_2 and qCO_2 (Table 2). Acetate was already formed at $D = 0.25$ h^{-1} and ethanol formation did set in at $D = 0.30$ h^{-1}, as compared with $D = 0.32$ h^{-1} and $D = 0.39$ h^{-1}, respectively, in cultures growing without propionate.

DISCUSSION

Regulation of respiration. Rieger et al. (43) have ascribed the long-term Crabtree effect in S. cerevisiae LBG H1022 to the existence of a limited respiratory capacity. The maximal oxidation capacity in this strain was only 8 mmol g (dry weight)$^{-1}$ h^{-1}. S. cerevisiae CBS 8066, however, exhibited an oxidation capacity of 12 mmol g (dry weight)$^{-1}$ h^{-1}. Such high rates of oxygen consumption were also observed with ethanol-limited cultures of our strain growing at dilution rates close to the μ_{max} of 0.21 h^{-1} (results not shown). A qO_2 of 12 mmol g^{-1} h^{-1} may thus be the intrinsic maximal respiratory capacity of S. cerevisiae CBS 8066. Approximately the same value for the maximal respiratory activity was observed for another strain of S. cerevisiae by Barford and Hall (3, 4).

In glucose-limited chemostat cultures of S. cerevisiae CBS 8066, the rate of oxygen consumption was linearly proportional to the dilution rate up to 0.30 h^{-1}. Above this dilution rate the oxygen consumption and carbon dioxide production rates increased unexpectedly (Fig. 2). The increased respiratory activity was reflected in a drop in cell yield. This lowered biomass yield could not be due to the loss of carbon via acid formation. The maximal amount of acetate present (0.7 mM) at these intermediary dilution rates was only 0.4% of the glucose input and an order of magnitude lower than the observed decrease in biomass yield. The disproportionality between respiratory activity and dilution rate at nonfermentative dilution rates was also observed by Barford and Hall (3, 4). These authors, however, did not pay attention to this peculiar pattern of respiratory activity at lower dilution rates. Rather, they focused on the respiratory activity of S. cerevisiae at higher dilution rates, when respiration and fermentation coexist. We observed that the enhanced respiration of glucose by S. cerevisiae coincided with the formation of acetate and pyruvate. Enhancement of respiration due to inhibitory concentrations of acetate was also observed for fed-batch growth of S. cerevisiae 264A (41). In that case, acetate formation coincided with ethanol formation, and the enhanced carbon dioxide production rates that accompanied the enhanced oxygen consumption rates were only attributed to the production of ethanol. The increase in respiration could also be explained by an uncoupling effect of acetate.

The similarity in the profiles of oxygen consumption and carbon dioxide production between our strain and that of Barford and Hall suggest that in their S. cerevisiae strain acetate formation did occur. The low concentrations of this metabolite may escape attention unless sensitive (enzymic)
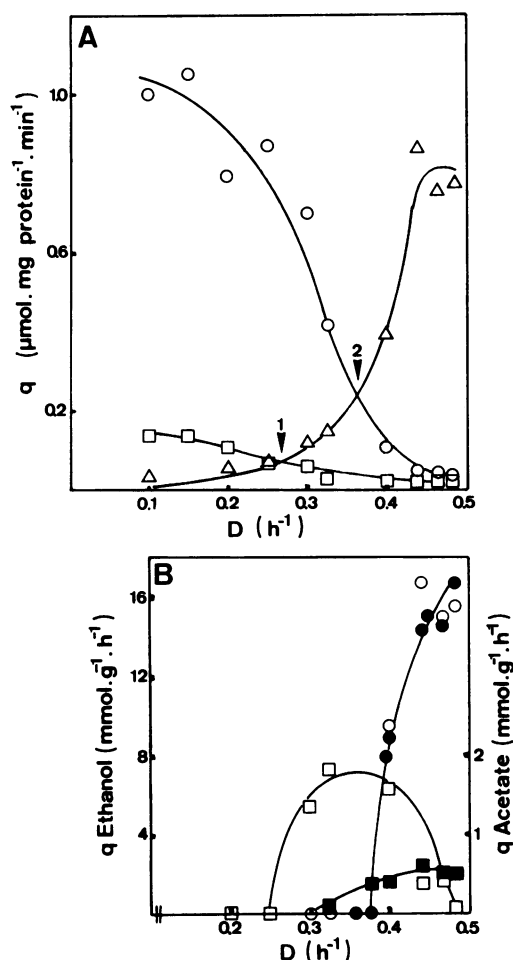

FIG. 6. In vivo activity (micromoles milligram of protein^{-1} minute^{-1}) of pyruvate decarboxylase ($\triangle$) and maximal activity of acetaldehyde dehydrogenases ($\bigcirc$) and acetyl-CoA synthetase ($\square$). 1, Dilution rate at which acetate formation has to set in. 2, Dilution rate at which ethanol formation has to set in. (B) Fluxes of ethanol ($\bullet$ and $\bigcirc$) and acetate ($\blacksquare$ and $\square$) (millimoles gram [dry weight]$^{-1}$ hour^{-1}) in glucose-limited chemostat cultures of S. cerevisiae CBS 8066. $\bullet$ and $\blacksquare$, Values observed in chemostat cultures. $\bigcirc$ and $\square$, Fluxes calculated on the basis of the in vivo pyruvate decarboxylase activity and the capacities of acetaldehyde dehydrogenases and acetyl-CoA synthetase.

TABLE 2. Influence of propionate on the steady-state behavior of *S. cerevisiae* CBS 8066

Culture	D (h^{-1})	qO_2 (mmol g^{-1} h^{-1})	qCO_2 (mmol g^{-1} h^{-1})	Cell yield (g [dry wt] g of glucose^{-1})	Glucose (mM)	Acetate (mM)	Ethanol (mM)
Glucose limited	0.25	6.5	6.9	0.50	0.09	0	0
	0.30	7.2	8.2	0.50	0.11	0	0
	0.32	9.2	9.3	0.50	0.12	0.20	0
	0.33[a]	9.2	9.1	0.49	0.07	0.23	0
Glucose limited plus 5 mM propionate	0.25	9.4	9.0	0.43	0.10	0.15	0
	0.30	12.3	12.2	0.36	0.11	0.48	0
	0.32	10.2	15.3	0.25	0.25	1.50	40
	0.33	9.7	16.9	0.23	0.31	1.80	60

[a] This culture had been pregrown at the same dilution rate in the presence of 5 mM propionate.

methods for its determination are used. Evidently, the growth rate at which alcoholic fermentation sets in may be strain dependent, as a result of different maximal respiratory capacities and acetate-producing abilities.

Weak acids may act as uncouplers (2, 7), and in yeasts weak organic acids may interfere with energy metabolism at two levels as a result of diffusion through membranes over which a proton motive force is present. Firstly, by dissipation of the proton motive force over the plasma membrane more ATP must be hydrolyzed by the ATPase to maintain the proton gradient. As a result, enhanced mitochondrial ATP synthesis and thus enhanced respiration are required. Secondly, direct uncoupling at the level of the inner mitochondrial membrane would negatively affect the proton-ATP stoichiometry and thus necessitate the oxidation of more reducing equivalents (enhanced respiration) to maintain the same rate of mitochondrial ATP production. As a result, enhanced respiration would again be required. That low concentrations of a weak organic acid indeed may have a drastic effect on energy metabolism in yeasts is substantiated by the experiments in which *S. cerevisiae* CBS 8066 was grown in the presence of propionate (Table 2). In these cultures the respiratory activity was strongly enhanced and was accompanied by a decrease in cell yield. It is significant that in this case acetate formation was observed, indicating that a high respiratory activity is intrinsically associated with acetate formation.

In glucose-limited cultures the highest steady-state rate of oxygen consumption was observed at $D = 0.38$ h^{-1} (Fig. 2 and 4A), whereas the same high respiration rate already was apparent at $D = 0.30$ h^{-1} when the yeast was grown in glucose-limited cultures in the presence of propionate (Table 2). Since in both cases alcoholic fermentation started when the dilution rate was increased further, it seems likely that the triggering of ethanol production is a consequence of reaching the limit of the respiratory capacity, as pointed out by Fiechter et al. (18). It should be stressed, however, that the maximal respiratory activity in glucose-limited cultures of *S. cerevisiae* CBS 8066 is reached "prematurely." From the rate of oxygen consumption at dilution rates below 0.30 h^{-1} (Fig. 2), it can be calculated that a qO_2 of 12 mmol g^{-1} h^{-1} should allow full respiratory metabolism up to a dilution rate of 0.48 h^{-1}, if the relationship between oxygen consumption and dilution rate in carbon-limited cultures is linear, as is usually observed. From the observation that alcoholic fermentation had already started at the lower dilution rate of 0.39 h^{-1} (Fig. 1), it can be concluded that the metabolic events (acid formation) triggering the enhanced respiration play a key role in the onset of alcoholic fermentation.

Multiple routes of pyruvate metabolism. The cause of acetate formation is the limiting capacity of the pyruvate dehydrogenase bypass (25). This route (Fig. 1) involves acetaldehyde and acetate as free intermediates and proceeds via pyruvate decarboxylase (EC 4.1.1.1), acetaldehyde dehydrogenases (EC 1.2.1.5 and EC 1.2.1.4), and acetyl-CoA synthetase (EC 6.2.1.1) (30). The physiological function of this bypass route in yeasts may be the generation of reducing equivalents (NADPH) for biosynthetic purposes (33, 35). If so, only the cytosolic enzyme would be functional in this respect, since the inner mitochondrial membrane is impermeable to reduced pyridine nucleotides (54). So far, shuttles for the export of NADPH from the mitochondria to the cytosol, where almost all NADPH consumption for biosynthetic purposes takes place (10, 22, 44, 57), have not been found.

It is well known that the hexose monophosphate pathway is the main source of NADPH in yeasts (10, 12, 21). Whether the decreased levels of the key enzyme of this pathway, glucose 6-phosphate dehydrogenase (Fig. 5C), reflect a decreased flux, thereby necessitating additional NADPH formation via acetaldehyde dehydrogenases, is not clear. It has been established that the onset of alcoholic fermentation is accompanied by elevated levels of glucose 6-phosphate (von Meyenburg, Ph.D. thesis). This may allow a high metabolic flux through the hexose monophosphate pathway despite a relatively low level of glucose 6-phosphate dehydrogenase.

Owing to the insufficient amount of acetyl-CoA synthetase present at dilution rates between 0.30 and 0.38 h^{-1}, acetate was produced. This situation is intermediate between strict oxidative metabolism (which occurs below $D = 0.30$ h^{-1}) and "oxido-reductive" metabolism (47) (which occurs above $D = 0.38$ h^{-1}). Qualitatively similar results have been obtained for another Crabtree-positive yeast, *Brettanomyces intermedius* CBS 1943 (50). In addition, three distinct metabolic situations have been encountered in glucose-limited chemostat cultures of this yeast: strictly respiratory metabolism at low dilution rates, respiration associated with acetate formation at intermediary dilution rates, and concurrent alcoholic fermentation and acetate formation at high dilution rates.

Chemostat cultivation is a necessity for the calculation of fluxes at branching points in metabolic pathways in microorganisms. Only in this way can a constant environment in which fluxes are constant in time be maintained. However, even with this technique the calculation of fluxes through branched pathways on the basis of biochemical data is rather complicated. Apart from the capacities of the systems as determined by enzyme assays under conditions of substrate excess, the kinetic constants of the enzymes and the con-

centrations of intracellular substrates, inhibitors, or activators should be precisely determined. With eucaryotes the situation is even more complex, owing to subcellular compartmentation (29) and the existence of isoenzymes. Isoenzymes of acetaldehyde dehydrogenases, alcohol dehydrogenase, and pyruvate decarboxylase have been reported to exist in S. cerevisiae (13, 27, 32, 36). Moreover, in the case of acetaldehyde and alcohol dehydrogenases, isoenzymes occur in different compartments (13, 27). Acetyl-CoA synthetase is a mitochondrial enzyme, but depending on the cultivation conditions, it can also be recovered in the microsomal fraction (30).

Despite these complications we attempted to explain the excretion of various metabolites in aerobic steady-state cultures of S. cerevisiae CBS 8066 on the basis of enzymological data. Rather than estimating the flux through each enzyme involved (Fig. 1), we estimated only the in vivo flux through pyruvate decarboxylase and related this to the maximal possible fluxes through the other enzymes. The calculation of the in vivo flux through pyruvate decarboxylase is relatively simple. The enzyme catalyzes a one-substrate reaction (6) and is exclusively located in the cytosol. Furthermore, the cytosolic concentration of phosphate, an allosteric inhibitor of the enzyme, has been determined via phosphorus nuclear magnetic resonance (17), whereas the intracellular pyruvate concentration may be calculated from the amount present in the culture fluid. Assuming an accumulation factor of 100, as derived from the ΔpH over the plasma membrane, the maximal internal concentration of pyruvate would be 40 mM. This value is in agreement with reported intracellular pyruvate concentrations of up to 10 mM in fermenting batch cultures (20, 45, 48). Below $D = 0.30\ h^{-1}$, the intracellular concentrations were calculated via extrapolation with a Hanes plot. If these values are real, it must be concluded that pyruvate decarboxylase is already operative at low dilution rates, when metabolite excretion does not occur. If it is assumed, on the basis of affinity constants (Table 1), that the acetaldehyde produced by pyruvate decarboxylase is preferentially oxidized to acetate, its conversion to acetyl-CoA would form a bottleneck above $D = 0.27\ h^{-1}$. Only when the flux of acetaldehyde to acetate through acetaldehyde dehydrogenases is saturated ($D = 0.37\ h^{-1}$) must ethanol formation set in as well. This pattern of metabolite production was indeed observed. Above $D = 0.30\ h^{-1}$, acetate was excreted by glucose-limited cultures of S. cerevisiae CBS 8066. Above $D = 0.38\ h^{-1}$, ethanol production occurred as well.

Crabtree effect. Our results have confirmed and extended previous observations (3, 5, 39, 43) on the triggering of alcoholic fermentation in aerobic sugar-limited chemostat cultures of S. cerevisiae. Particularly striking in this respect are the data from shift experiments. More than 25 volume changes were required for the establishment of a steady state. From the patterns of oxygen consumption and carbon dioxide production (Fig. 4A) it can be concluded that this unusually long adaptation primarily consists of an increase in fermentative capacity at the expense of biomass formation. In summary, it is postulated that the onset of alcoholic fermentation is a consequence of the in vivo functioning of the pyruvate dehydrogenase bypass route. Owing to glucose repression at high growth rates, the amount of acetyl-CoA synthetase is insufficient for the complete functioning of the pyruvate dehydrogenase bypass. The nonmetabolized, accumulated acetic acid uncouples respiration, as reflected by the enhanced qO_2. As a result, at a dilution rate of $0.38\ h^{-1}$ maximal ATP production (maximal oxidation capacity) by

the mitochondria is reached. To grow faster (that is, at a higher dilution rate) the organism must generate additional ATP by the fermentative pathway. This is accomplished via an increase in the amount of pyruvate decarboxylase (Fig. 5A). It would therefore be of interest to study the effects of enhancing the synthesis of acetyl-CoA synthetase via genetic manipulation, since this might prevent the accumulation of acetate.

LITERATURE CITED

1. **Addanki, S., F. D. Cahill, and J. F. Sotos.** 1968. Determination of intramitochondrial pH and intramitochondrial-extramitochondrial pH gradient of isolated heart mitochondria by the use of 5,5-dimethyl-2,4-oxazolidinedione. J. Biol. Chem. **243:**2337–2348.
2. **Alexander, B., S. Leach, and W. J. Ingledew.** 1987. The relationship between chemiosmotic parameters and sensitivity to anions and organic acids in the acidophile Thiobacillus ferrooxidans. J. Gen. Microbiol. **133:**1171–1179.
3. **Barford, J. P., and R. J. Hall.** 1979. An examination of the Crabtree effect in Saccharomyces cerevisiae: the role of respiratory adaptation. J. Gen. Microbiol. **114:**267–275.
4. **Barford, J. P., and R. J. Hall.** 1981. A mathematical model for the aerobic growth of Saccharomyces cerevisiae with a saturated respiratory capacity. Biotechnol. Bioeng. **23:**1735–1762.
5. **Barford, J. P., P. M. Jeffery, and R. J. Hall.** 1981. The Crabtree effect in Saccharomyces cerevisiae—primary control mechanism or transient? p. 255–260. In M. Moo-Young, C. W. Robinson, and C. Vezina (ed.), Advances in biotechnology, vol. 1. Pergamon Press, Toronto.
6. **Barman, T. E.** 1974. Enzyme handbook. Supplement I, p. 701. Springer-Verlag KG, Berlin.
7. **Baronofsky, J. J., W. J. A. Schreurs, and E. R. Kashket.** 1984. Uncoupling by acetic acid limits growth of and acetogenesis by Clostridium thermoaceticum. Appl. Environ. Microbiol. **48:**1134–1139.
8. **Beck, C., and H. K. von Meyenburg.** 1968. Enzyme pattern and aerobic growth of Saccharomyces cerevisiae under various degrees of glucose limitation. J. Bacteriol. **96:**479–486.
9. **Boiteux, A., and B. Hess.** 1970. Allosteric properties of yeast pyruvate decarboxylase. FEBS Lett. **9:**293–296.
10. **Botham, P. A., and C. Radledge.** 1979. A biochemical explanation for lipid accumulation in Candida 107 and other oleaginous micro-organisms. J. Gen. Microbiol. **114:**361–375.
11. **Bruinenberg, P. M., J. P. van Dijken, and W. A. Scheffers.** 1983. An enzymic analysis of NADPH production and consumption in Candida utilis CBS 621. J. Gen. Microbiol. **129:**965–971.
12. **Bruinenberg, P. M., J. P. van Dijken, and W. A. Scheffers.** 1983. A theoretical analysis of NADPH production and consumption in yeasts. J. Gen. Microbiol. **129:**953–964.
13. **Carrascosa, J. M., M. D. Viguera, I. Núñez de Castro, and W. A. Scheffers.** 1981. Metabolism of acetaldehyde and Custers effect in the yeast Brettanomyces abstinens. Antonie van Leeuwenhoek J. Microbiol. **47:**209–215.
14. **Crabtree, H. G.** 1929. Observations on the carbohydrate metabolism of tumours. Biochem. J. **23:**536–545.
15. **De Deken, R. H.** 1966. The Crabtree effect: a regulatory system in yeast. J. Gen. Microbiol. **44:**149–156.
16. **de la Peña, P., F. Barros, S. Gascón, S. Ramos, and P. S. Lazo.** 1982. The electrochemical proton gradient of Saccharomyces. The role of potassium. Eur. J. Biochem. **123:**447–453.
17. **den Hollander, J. A., K. Ugurbil, T. R. Brown, and R. G. Shulman.** 1981. Phosphorus-31 nuclear magnetic resonance studies of the effect of oxygen upon glycolysis in yeast. Biochemistry **20:**5871–5880.

18. **Fiechter, A., G. F. Fuhrmann, and O. Käppeli.** 1981. Regulation of glucose metabolism in growing yeast cells. Adv. Microb. Physiol. **22:**123–183.

19. **Frenkel, E. P., and R. L. Kitchens.** 1981. Acetyl-CoA synthetase from bakers' yeast (*Saccharomyces cerevisiae*). Methods Enzymol. **71:**317–324.

20. **Gancedo, J. M., and C. Gancedo.** 1973. Concentrations of intermediary metabolites in yeast. Biochimie **55:**205–211.

21. **Gancedo, J. M., and R. Lagunas.** 1973. Contribution of the pentose-phosphate pathway to glucose metabolism in *Saccharomyces cerevisiae*: a critical analysis on the use of labelled glucose. Plant Sci. Lett. **1:**193–200.

22. **Gumaa, K. A., A. L. Greenbaum, and P. McLean.** 1973. Adaptive changes in satellite systems related to lipogenesis in rat and sheep mammary gland and in adipose tissue. Eur. J. Biochem. **34:**188–198.

23. **Harder, W., K. Visser, and J. G. Kuenen.** 1974. Laboratory fermentor with an improved magnetic drive. Lab. Pract. **23:**644–645.

24. **Holzer, H.** 1961. Regulation of carbohydrate metabolism by enzyme competition. Cold Spring Harbor Symp. Quant. Biol. **26:**277–288.

25. **Holzer, H., and H. W. Goedde.** 1957. Zwei Wege von Pyruvat zu Acetyl-Coenzym A in Hefe. Biochem. Z. **329:**175–191.

26. **Hübner, G., R. Weidhase, and A. Schellenberger.** 1978. The mechanism of substrate activation of pyruvate decarboxylase: a first approach. Eur. J. Biochem. **92:**175–181.

27. **Jacobson, M. K., and C. Bernofsky.** 1974. Mitochondrial acetaldehyde dehydrogenase from *Saccharomyces cerevisiae*. Biochim. Biophys. Acta **350:**277–291.

28. **Käppeli, O.** 1986. Regulation of carbon metabolism in *Saccharomyces cerevisiae* and related yeasts. Adv. Microb. Physiol. **28:**181–209.

29. **Keech, D. B., and J. C. Wallace (ed.).** 1985. Pyruvate carboxylase, p. 23–27. CRC Press, Inc., Boca Raton, Fla.

30. **Klein, H. P., and L. Jahnke.** 1971. Variations in the localization of acetyl-coenzyme A synthetase in aerobic yeast cells. J. Bacteriol. **106:**596–602.

31. **Kresze, G.-B., and H. Ronft.** 1981. Pyruvate dehydrogenase complex from baker's yeast. I. Purification and some kinetic and regulatory properties. Eur. J. Biochem. **119:**573–579.

32. **Kuo, D. J., G. Dikdan, and F. Jordan.** 1986. Resolution of brewers' yeast pyruvate decarboxylase into two isozymes. J. Biol. Chem. **261:**3316–3319.

33. **Lagunas, R., and J. M. Gancedo.** 1973. Reduced pyridine-nucleotides balance in glucose-growing *Saccharomyces cerevisiae*. Eur. J. Biochem. **37:**90–94.

34. **LaNoue, K. F., and A. C. Schoolwerth.** 1979. Metabolite transport in mitochondria. Annu. Rev. Biochem. **48:**871–922.

35. **Llorente, N., and I. Núñez de Castro.** 1977. Physiological role of yeasts $NAD(P)^+$- and $NADP^+$-linked aldehyde dehydrogenases. Rev. Esp. Fisiol. **33:**135–142.

35a. **Lowry, O. H., N. J. Rosebrough, A. L. Farr, and R. J. Randall.** 1951. Protein measurement with the Folin phenol reagent. J. Biol. Chem. **193:**265–275.

36. **Lutstorf, U., and R. Megnet.** 1968. Multiple forms of alcohol dehydrogenase in *Saccharomyces cerevisiae*. Arch. Biochem. Biophys. **126:**933–944.

37. **Nicolay, K., W. A. Scheffers, P. M. Bruinenberg, and R. Kaptein.** 1982. Phosphorus-31 nuclear magnetic resonance studies of intracellular pH, phosphate compartmentation and phosphate transport in yeasts. Arch. Microbiol. **133:**83–89.

38. **Parulekar, S. J., G. B. Semones, M. J. Rolf, J. C. Lievense, and H. C. Lim.** 1986. Induction and elimination of oscillations in continuous cultures of *Saccharomyces cerevisiae*. Biotechnol. Bioeng. **28:**700–710.

39. **Petrik, M., O. Käppeli, and A. Fiechter.** 1983. An expanded concept for the glucose effect in the yeast *Saccharomyces uvarum*: involvement of short- and long-term regulation. J. Gen. Microbiol. **129:**43–49.

40. **Polakis, E. S., W. Bartley, and G. A. Meak.** 1965. Changes in the activities of respiratory enzymes during the aerobic growth of yeast on different carbon sources. Biochem. J. **97:**298–302.

41. **Pons, M.-N., A. Rajab, and J.-M. Engasser.** 1986. Influence of acetate on growth kinetics and production control of *Saccharomyces cerevisiae* on glucose and ethanol. Appl. Microbiol. Biotechnol. **24:**193–198.

42. **Postma, E., W. A. Scheffers, and J. P. van Dijken.** 1988. Adaptation of the kinetics of glucose transport to environmental conditions in the yeast *Candida utilis* CBS 621: a continuous-culture study. J. Gen. Microbiol. **134:**1109–1116.

43. **Rieger, M., O. Käppeli, and A. Fiechter.** 1983. The role of a limited respiration in the incomplete oxidation of glucose by *Saccharomyces cerevisiae*. J. Gen. Microbiol. **129:**653–661.

44. **Ryan, E. D., and G. B. Kohlhaw.** 1974. Subcellular localization of isoleucine-valine biosynthetic enzymes in yeast. J. Bacteriol. **120:**631–637.

45. **Sáez, M. J., and R. Lagunas.** 1976. Determination of intermediary metabolites in yeast. Critical examination of the effect of sampling conditions and recommendations for obtaining true levels. Mol. Cell. Biochem. **13:**73–78.

46. **Sharma, S., and P. Tauro.** 1986. Control of ethanol production by yeast: role of pyruvate decarboxylase and alcohol dehydrogenase. Biotechnol. Lett. **8:**735–738.

47. **Sonnleitner, B., and O. Käppeli.** 1986. Growth of *Saccharomyces cerevisiae* is controlled by its limited respiratory capacity: formulation and verification of a hypothesis. Biotechnol. Bioeng. **28:**927–937.

48. **Trevelyan, W. E., and J. S. Harrison.** 1954. Studies on yeast metabolism. 3. The intracellular level of pyruvate during yeast fermentation. Biochem. J. **57:**556–561.

49. **Valle, E., L. Bergillos, S. Gascón, F. Parra, and S. Ramos.** 1986. Trehalase activation in yeasts is mediated by an internal acidification. Eur. J. Biochem. **154:**247–251.

50. **van Dijken, J. P., and W. A. Scheffers.** 1986. Redox balances in the metabolism of sugars by yeasts. FEMS Microbiol. Rev. **32:**199–224.

51. **Verduyn, C., G. J. Breedveld, W. A. Scheffers, and J. P. van Dijken.** 1988. Substrate specificity of alcohol dehydrogenase from the yeasts *Hansenula polymorpha* CBS 4732 and *Candida utilis* CBS 621. Yeast **4:**143–148.

52. **Verduyn, C., J. P. van Dijken, and W. A. Scheffers.** 1984. Colorimetric alcohol assays with alcohol oxidase. J. Microbiol. Methods **2:**15–25.

53. **Verduyn, C., T. P. L. Zomerdijk, J. P. van Dijken, and W. A. Scheffers.** 1984. Continuous measurement of ethanol production by aerobic yeast suspensions with an enzyme electrode. Appl. Microbiol. Biotechnol. **19:**181–185.

54. **von Jagow, G., and M. Klingenberg.** 1970. Pathways of hydrogen in mitochondria of *Saccharomyces carlsbergensis*. Eur. J. Biochem. **12:**583–592.

55. **von Meyenburg, H. K.** 1969. Energetics of the budding cycle of *Saccharomyces cerevisiae* during glucose limited aerobic growth. Arch. Mikrobiol. **66:**289–303.

56. **Washburn, E. W. (ed.).** 1929. International critical tables of numerical data, physics, chemistry and technology, vol. 6, p. 263. McGraw-Hill Book Co., New York.

57. **Wipf, B., and T. Leisinger.** 1977. Compartmentation of arginine biosynthesis in *Saccharomyces cerevisiae*. FEMS Microbiol. Lett. **2:**239–242.

58. **Witt, I., R. Kronau, and H. Holzer.** 1966. Repression von Alcoholdehydrogenase, Malatdehydrogenase, Isocitratlyase und Malatsynthase in Hefe durch Glucose. Biochim. Biophys. Acta **118:**522–537.